Chemical Engineering Science, Vol. 44, No. 3, pp. 703–712, 1989.
Printed in Great Britain.

0009–2509/89 $3.00 + 0.00

USE OF AN AXIAL-DISPERSION MODEL FOR KINETIC DESCRIPTION OF HYDROCRACKING

RAJAMANI KRISHNA and ALOK K. SAXENA
Indian Institute of Petroleum, Dehra Dun 248005, India

(*Received* 22 *March* 1988; *accepted for publication* 10 *August* 1988)

Abstract—A novel approach to the description of the kinetics of hydrocracking of vacuum gas oils (VGO) is developed, in which the progress of cracking with increasing space time is modeled by the consideration of two aspects: (i) the distribution of boiling point around the mid-boiling temperature T_{50}, and (ii) the decay kinetics of T_{50}. Using the data of Bennett and Bourne (1972) for the hydrocracking of Kuwait VGO it is shown that the distribution of boiling points around T_{50}, after appropriate scaling, can be adequately described by an axial-dispersion model. To gain an insight into the physico-chemical basis of the axial-dispersion parameter Pe, and the kinetics decay of T_{50}, a detailed kinetic model is also developed for hydrocracking, consisting of lumped species: paraffins, naphthenes, aromatics and sulphur compounds. The rate constants for the detailed reaction network for various cuts were determined from pilot plant data for Kuwait VGO reported by Bennett and Bourne (1972). With the aid of the detailed kinetic model, verified for its predictive capability by testing with two other feedstocks, it is shown that the axial-dispersion parameter Pe is almost solely governed by the paraffinicity of the feedstock and may be considered to reflect the "selectivity" of the catalyst. The decay order of T_{50}, n, and the corresponding decay rate constant, k_{50}, are also found to be primarily governed by the feed paraffinicity; the decay order n varies from nearly second-order for feedstocks with extremely low paraffin content to approximately first-order for highly paraffinic feeds. Together, these two parameters, n and k_{50}, portray the "activity" of the catalyst.

INTRODUCTION

For the description of the kinetics of the hydrocracking of vacuum gas oils (VGO) or residues, two approaches are prevalent in the literature. In the first approach some form of lumping is employed with respect to both the compound types present in the feedstock and the product boiling ranges of interest [e.g. Tom *et al.* (1972)]; the advantage of using this kinetic model, which differentiates between different compound types and different boiling ranges of interest, is the promise of a predictive capability for dealing with feedstocks other than the one for which the data have been generated. The second, more simple, approach to the description of the kinetics of hydrocracking is suggested by Strangeland (1974) who uses the analogy of cracking with comminution to develop a correlative method for predicting the entire true boiling point (TBP) curve of the product for a specified set of operating conditions.

The present approach to the kinetic description of hydrocracking is fundamentally different from the earlier published models and is based on the concept of axial dispersion. The task was set of predicting the yields of various boiling range products with the minimum number of physically meaningful and interpretable parameters. Further, the model is required to have an in-built capability of differentiating between various feedstocks, catalysts and reaction temperature and pressure conditions.

CRACKING VIEWED AS ALTERATION OF THE MOLECULAR WEIGHT DISTRIBUTION

The cracking process is viewed as an alteration in the distribution of the molecular weights. This latter distribution is related to the distribution of boiling points [cf. Maxwell (1965) which shows the linear dependence of the boiling point of hydrocarbons on the average molecular weight of that fraction]; it is conventional in petroleum technology to use the TBP curve to represent this distribution. Figure 1 shows the TBP curves for Kuwait VGO feed and the hydrocrackate products at four different space times [data from Bennett and Bourne (1972)] and it is apparent that there is an alteration in the boiling point distributions around the mean, T_{50}. With increased residence time, the average molecular weight of the product decreases; this is refelected in the decrease in the mid-boiling temperature T_{50} (cf. Fig. 1).

Now, in physical dispersion of say a ramp tracer input, the cross-sectional mean concentration of the tracer at the plane moving with average axial velocity remains constant while its distribution increases with the length of the conduit (increasing residence time). In contrast, hydrocracking results in a decrease in the mean concentration (i.e. molecular weight or, equivalently, boiling temperature). It may therefore be expected that, if the analogy of hydrocracking with physical dispersion is to be drawn, the distribution of the molecular weights (equivalent to the boiling point distributions) of the hydrocrackates at different space times must be normalized around the respective means of the distributions. Since, in hydrocracking, the objective is to crack heavier molecules into lighter ones, it is decided to normalize the distributions (i.e. the TBP curves) as follows:

$$T^* = \frac{\mathrm{FBP}_f - T}{\mathrm{FBP}_f - T_{50}} \tag{1}$$

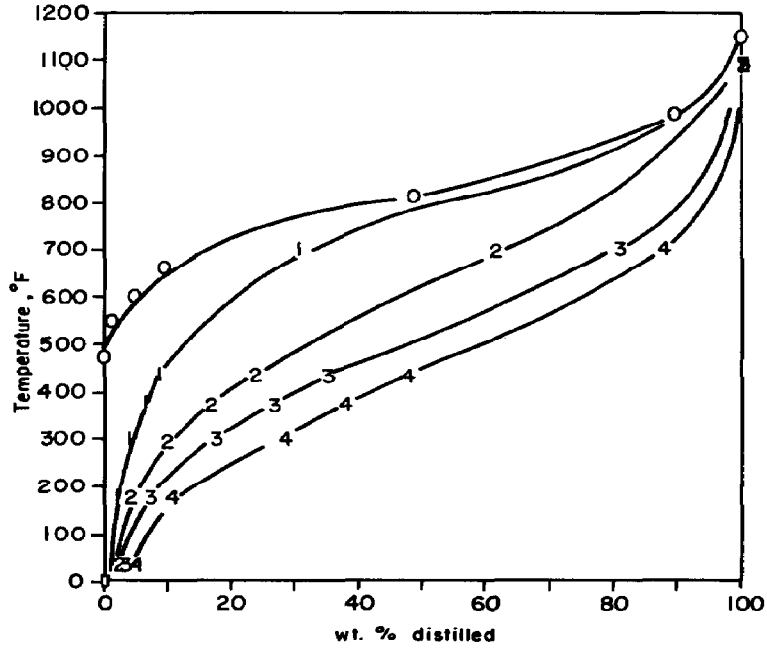

Fig. 1. TBP curves for Kuwait VGO (marked 0) and hydrocracked products obtained at various severity levels (marked 1, 2, 3 and 4 corresponding to space times of 0.383, 0.952, 1.724 and 2.5 h, respectively). The data have been taken from Bennett and Bourne (1972). In the case of the feedstock the TBP has been calculated from the reported Engler vacuum distillation data. For the hydrocracked products, the TBP curve has been generated from the actual product yields.

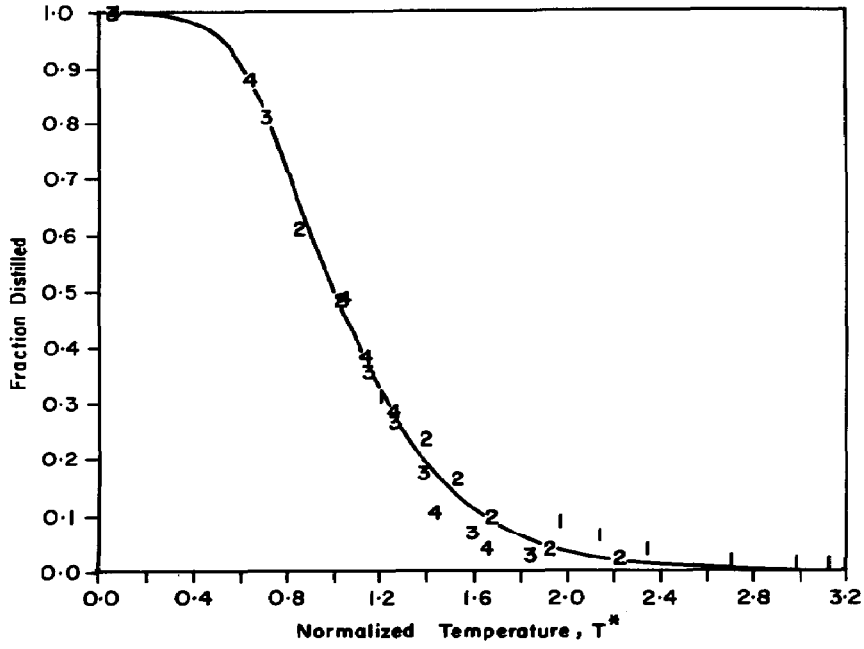

Fig. 2. Normalized TBP curve for hydrocracking of Kuwait VGO based on the data presented in Fig. 1. The dimensionless temperature T^* has been calculated from eq. (1) with the FBP of the feed taken as 1200°F. The T_{50} for the products were obtained from Fig. 1. The smooth curve was obtained using eq. (2), taking $Pe = 14$.

where FBP_f is the final boiling point of the feedstock. With the normalized temperature as defined in eq. (1), the TBP curves for the four hydrocrackates all fall on the same curve (see Fig. 2). Also shown in Fig. 2 is a smooth curve using the conventional axial-dispersion model for dispersion in a tube with open boundaries at each end [e.g. see Smith (1981)]:

$$f = \frac{1}{2} + \frac{1}{2}\,\mathrm{erf}\left(\frac{1-T^*}{2T^{*1/2}}\,Pe^{1/2}\right) \qquad (2)$$

taking the axial-dispersion parameter Pe as 14. The RMSD of the fit of eq. (1) with the TBP data of Fig. 1 is 0.031, which can be considered to be very good. For predicting the yield of any particular boiling range cut, it remains to predict the value of T_{50} at the specified residence time. Figure 3 shows the plot of the T_{50} vs space time and it is seen that T_{50} decay appears to follow first-order kinetics:

$$T_{50,\tau} = T_{50,f} \exp(-k_{50}\tau). \quad (3)$$

This is not altogether an unexpected result in view of the fact that for a given boiling range cut the mean molecular weight is linearly dependent on the mean boiling point (Maxwell, 1965) and it is expected that the crackability of a molecule is dependent on its size, i.e. larger molecules crack more easily than smaller molecules. The first-order decay constant k_{50} was found by regression analysis to be 0.24 h^{-1} for Kuwait VGO feedstock. Later on in this paper the factors which determine the decay order of the mid-boiling temperature T_{50} will be examined in detail.

COMPARISON WITH A DETAILED KINETIC MODEL

The major merit in the dispersion model developed above is that the entire progression of the boiling point distributions with space time can be monitored by only two parameters: Pe and k_{50}. For a given catalyst and operating conditions, these two parameters must depend on the feedstock type and this dependence is investigated in the following by the aid of a detailed kinetic model. A model is set up as depicted in Fig. 4 wherein seven compound types ("lumps") are considered; for any given "cut" temperature, T_{cut}, the various compound types are distributed between the heavier (T^{+}_{cut}) and lighter (T^{-}_{cut}) fractions. Data on the compound type distributions, for the hydrocracking of Kuwait VGO, for various cuts (700, 437, 375, 300, 180 and 32°F) have been given by Bennett and Bourne (1972). Since the maximum cut temperature for which data are available is 700°F, sulphur compounds have been assumed to be present only in the heavier cut and the reaction scheme depicted in Fig. 4 conforms with the chemistry of hydrocracking as discussed in, for example, Langlois and Sullivan (1969). Assuming first-order kinetics for each reaction, and isothermal conditions [this condition was largely maintained in the experiments of Bennett and Bourne (1972)], the product distributions (expressed in weight percent) for each lump can be calculated for any given space time, τ, from the expressions given in Appendix A.

The 10 rate constants describing the reaction network in Fig. 4, $k_1, k_2, \ldots k_{10}$, were estimated for each of the six cuts (700, 437, 375, 300, 180 and 32°F) from the data of Bennett and Bourne (1972) for hydrocracking of Kuwait VGO at four different severity levels (space times of 0.383, 0.952, 1.724 and 2.5 h). The

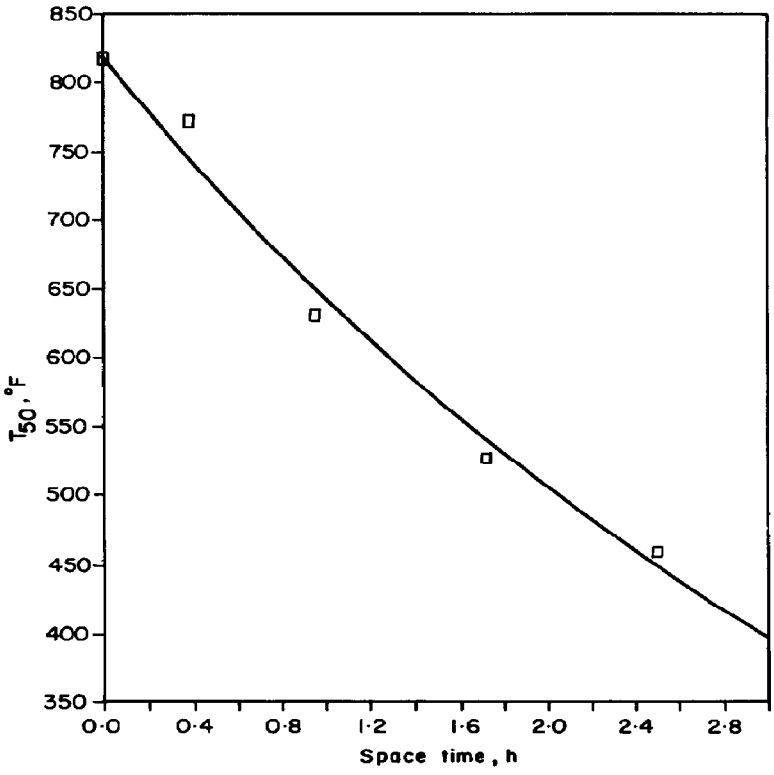

Fig. 3. Variaton of T_{50} with reaction severity for Kuwait VGO feedstock. Data taken from Bennett and Bourne (1972). The smooth curve is drawn using eq. (3), taking $k_{50} = 0.24\ h^{-1}$.

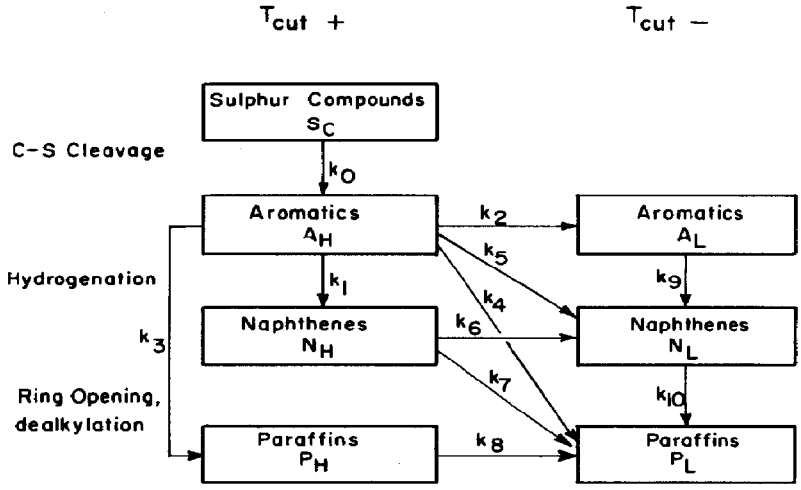

Fig. 4. Lumped reaction kinetic scheme for hydrocracking.

Table 1. First-order rate constants for the reaction network of Fig. 4 (h^{-1})†

	T_{cut} (°F)					
	700	437	375	300	180	32
k_0	8.3000	8.3000	8.3000	8.3000	8.3000	8.3000
k_1	1.2633	0.4943	0.4799	0.4624	0.4345	0.4000
k_2	0.6042	0.1809	0.1105	0.0397	0.0034	0.0000
k_3	0.0421	0.3131	0.2719	0.2593	0.2501	0.2302
k_4	0.5309	0.0211	0.0096	0.0095	0.0095	0.0095
k_5	0.0397	0.0383	0.0249	0.0131	0.0086	0.0000
k_6	1.1855	0.2772	0.2134	0.1117	0.0073	0.0000
k_7	0.1619	0.0474	0.0275	0.0275	0.0275	0.0275
k_8	0.4070	0.2391	0.1993	0.1518	0.0978	0.0299
k_9	0.2909	0.5434	0.5219	0.4509	0.4391	—
k_{10}	0.0818	0.0740	0.0709	0.0618	0.0608	—

† Estimated from the data of Bennett and Bourne (1972) for the hydrocracking of Kuwait VGO.

parameters were estimated using the Box–Simplex technique for minimizing the deviations between model and experiment. The estimated rate constants are given in Table 1 for the six cut temperatures. With the parameters thus estimated the kinetic expressions given in Appendix A could reproduce experimentally reported data on yields within a maximum error of 4%, which can be considered to be reasonably good. It was also noted that the error in the predictions of the detailed kinetic model did not vary with the cut temperature, pointing to the applicability of the kinetic model of Fig. 4 for any cut temperature.

With the set of parameters thus estimated, the TBP curve for the product obtained at any space time can be calculated. Figure 5 compares the yields for 700°F+, 300–700°F and 300°F− obtained experimentally for Kuwait VGO with the predictions of both the dispersion model [eqs (1)–(3), taking $Pe=14$ and $k_{50}=0.24\ h^{-1}$] and the detailed kinetic model (Fig. 4 with rate constants given in Table 1). It is observed that the simple dispersion model, with only two parameters, does a simulation job with an accuracy comparable to the detailed kinetic model employing 60 rate constants! The point emphasized with the results portrayed in Fig. 5 is that there is no apparent sacrifice in prediction accuracy if one opts for the simple, and physically appealing, dispersion model.

While the success obtained above pertained to yields of broad cuts, a word of caution is in order concerning the accuracy of prediction of yields of narrow cuts. Figure 6 compares the experimentally obtained yields of the 300–437 and 437–700°F fractions for hydrocracking of Kuwait VGO with those predicted by the dispersion model and the detailed kinetic model. The comparitively poorer accuracy of prediction in the yields of the narrower cuts is apparent but still the predicted results are within about 8% of the measured yields. It can be further seen that the both the dispersion model and the detailed kinetic model are of comparable accuracy.

PREDICTION OF THE YIELD STRUCTURE FOR ANY FEEDSTOCK

In the foregoing the applicability of the dispersion model to represent the hydrocracking process for one

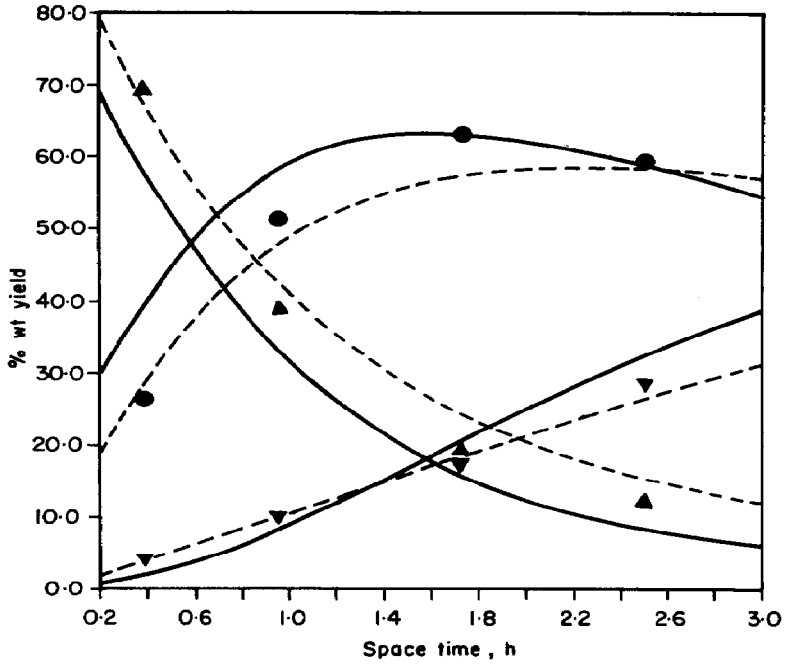

Fig. 5. Yields of 700°F+ (▲), 300–700°F (●), and 300°F− (▼) fractions on hydrocracking of Kuwait VGO; comparison of pilot plant experimental data of Bennett and Bourne (1972) with the predictions of both the dispersion model (——) and the detailed kinetic model (– – – – –).

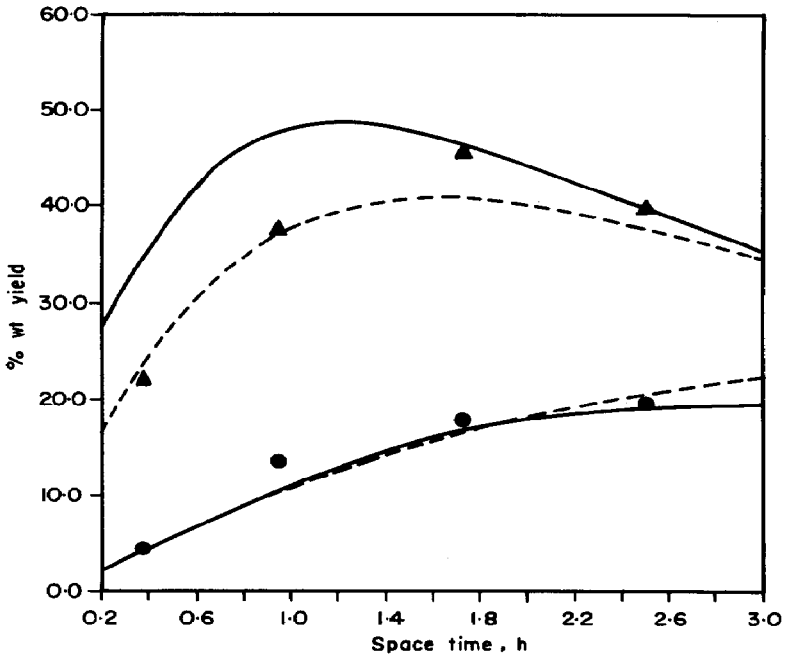

Fig. 6. Yields of 300–437°F (●) and 437–700°F (▲) fractions; comparison of simulations using the dispersion model (——) and the detailed kinetic model (– – – – –) with pilot plant experimental data of Bennett and Bourne (1972).

feedstock, Kuwait VGO, has been verified. The question remains about the dependence of the parameters Pe and k_{50} on the feedstock composition. In order to obtain an insight into this dependence one needs to depend on the ability of the detailed kinetic model, along with the rate constants of Table 1, to describe the behaviour of other feedstocks, albeit for the same catalyst and operating conditions of temperature and pressure. First, the predictive capability of the detailed kinetic model is verified by comparing the predictions

with the yields obtained with Iranian Light and Libyan VGO feedstocks (at a space time of 2.5 h), as also reported by Bennett and Bourne (1972), with the same catalyst and nearly identical temperature and pressure conditions; the experimental and predicted TBP curves are in extremely good agreement, verifying the predictive ability of the detailed kinetic model (see Fig. 7). In predicting the TBP curves shown in Fig. 7 the rate constants at an intermediate cut temperature of 550°F have been interpolated and it has been further assumed that the constants derived for $T_{cut} = 700$°F also hold for higher-temperature cuts of 850 and 1000°F.

Having verified the capability of the detailed kinetic model to describe the yield structure for any feedstock, one is now in a position to examine the dependence of Pe and the T_{50} decay constant on the feedstock composition. A set of simulations with the detailed kinetic model were carried out wherein the feedstock composition (paraffins, naphthenes and aromatics) were varied systematically within the range 20 to 60 wt %. Further, the TBP of the feedstock was also varied by choosing a range of dispersion parameters, $12 < Pe_f < 20$, with the mid-boiling temperature of the feed varying in the range 800–830°F. The FBP of the feed was maintained at 1200°F. For any given feedstock type and TBP, the use of the detailed kinetic model allowed the determination of the TBP of the hydrocracked product at any space time τ. In this manner the TBP curve of the hydrocrackates at various space times, $0.2 < \tau < 3$ h, were generated. Each of the set of TBP curves thus obtained at different space times can be normalized according to eq. (1). The best-fit value of the dispersion parameter Pe in eq. (2) was determined for each normalized hydrocrackate TBP curve. The variation of Pe with space time for one particular choice of feedstock ($Pe = 16$; paraffins = 40%, naphthenes = 30%, aromatics = 30%; $T_{50,f} = 820$°F) is shown in Fig. 8. An initial decrease in Pe (i.e. broadening of the TBP curve) followed by a small increase (i.e. narrowing of the TBP curve) was observed in all the simulations with different feedstocks. In spite of this variation in Pe, all the normalized TBP curves from a given feedstock can, without significant loss in accuracy, be represented by a single value of Pe (13.8) as shown in Fig. 9 for the above-mentioned feedstock. It is heartening, again, to note that the dispersion model, with a single dispersion parameter Pe, is able to reproduce the boiling point distributions of the various hydrocrackates with good accuracy (the RMSD of the fit is 0.038).

For several feedstock compositions, with varying TBP, the values of the "best-fit" dispersion parameter, obtained in the manner illustrated by Fig. 9, were

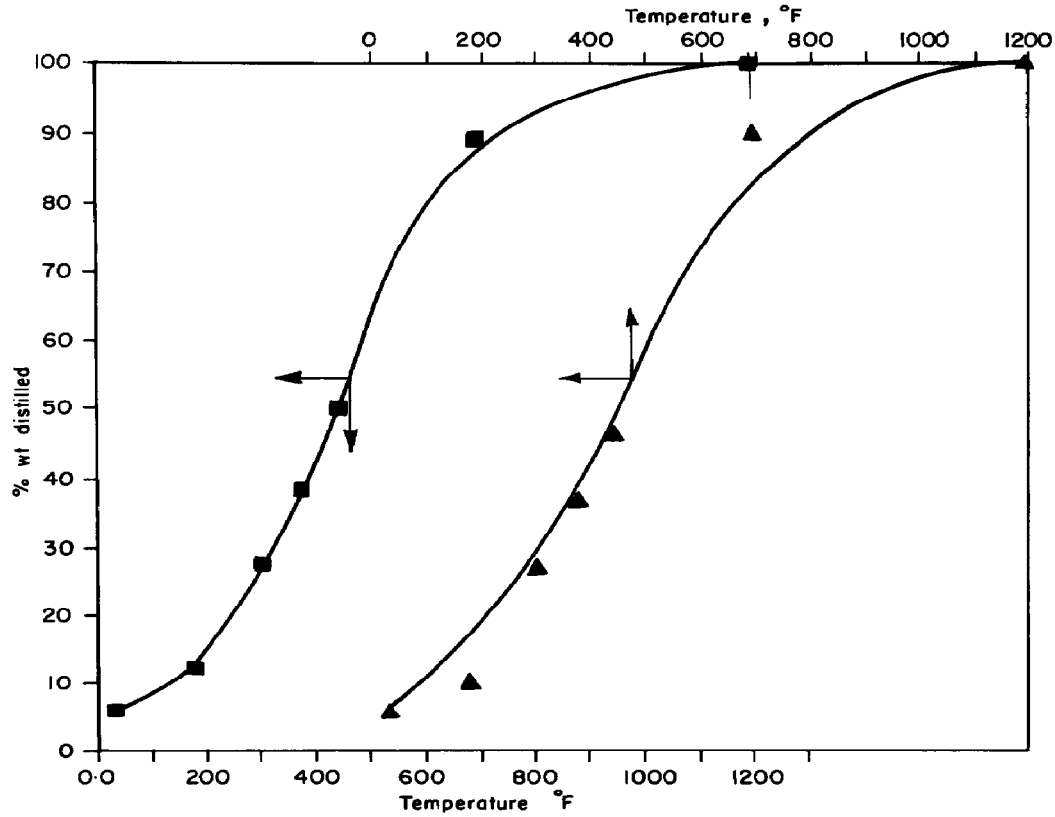

Fig. 7. TBP curves for hydrocracked products obtained from Iran Light (■) and Libyan (▲) feedstocks. Comparison of kinetic model predictions (——) with the data reported by Bennett and Bourne (1972) for a space time of 2.5 h.

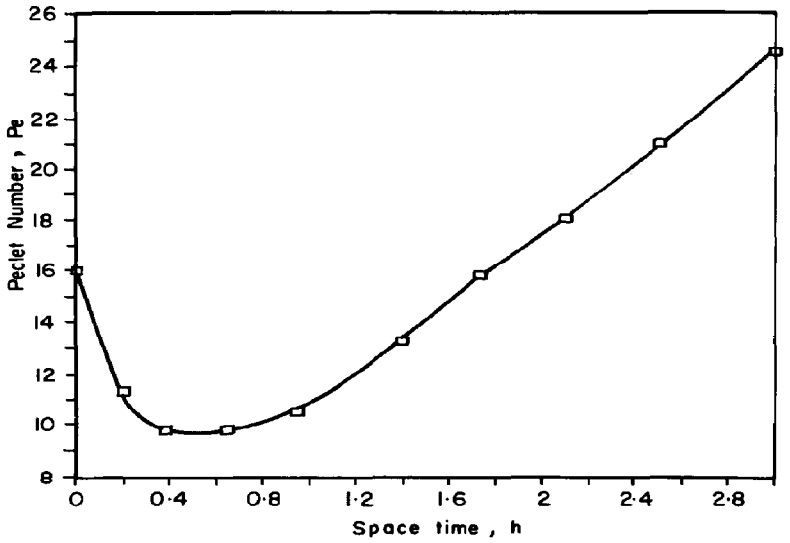

Fig. 8. Variation of dispersion parameter Pe of hydrocrackates with space time for a feedstock: $Pe_f = 16$, paraffins 40%, naphthenes = 30%, aromatics = 30%, $T_{50,f} = 820°F$, $FBP_f = 1200°F$.

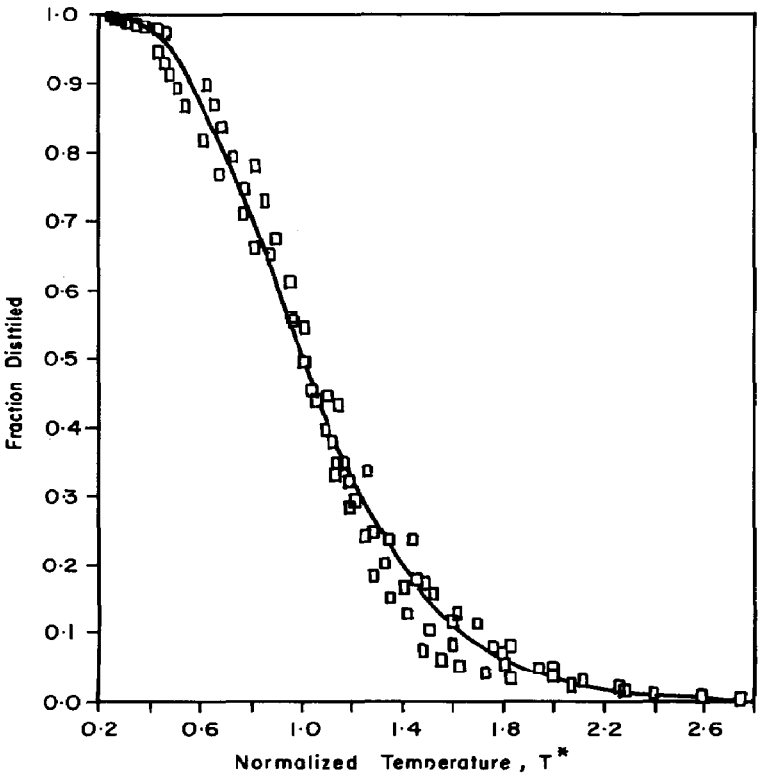

Fig. 9. Normalized TBP curves for hydrocrackate, obtained using kinetic model for the feedstock described in Fig. 8 at space times of 0.2, 0.383, 0.6, 0.952, 1.4, 1.724, 2.1, 2.5 and 3.0 h. The smooth curve has been drawn using eq. (2), taking $Pe = 13.8$.

found to depend only on the feedstock paraffinicity and fairly insensitive to the naphthene/aromatic ratio. Also, interestingly, the value of Pe for any given paraffinicity was not affected by Pe_f, i.e. the boiling point distribution of the feed; these results are shown in Fig. 10. An increase in the feed paraffinicity results in a lowered value of Pe which signifies a broader distribution of boiling temperatures (or, equivalently,

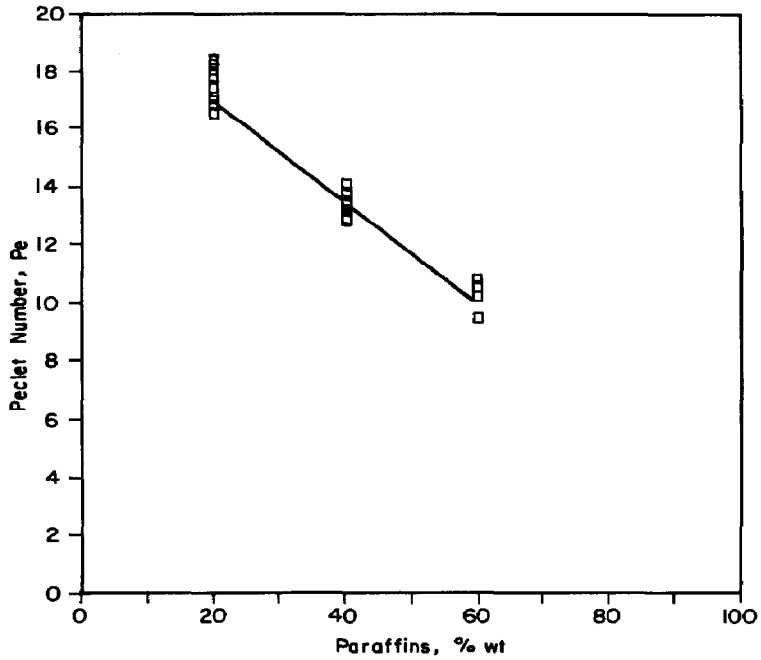

Fig. 10. Dependence of dispersion parameter Pe on feedstock paraffinicity.

molecular weights) around the mean. A simple linear correlation:

$$Pe = 20.125 - 0.175(\text{wt \% paraffins in feed}) \quad (4)$$

can be used for *a priori* predictions of the dispersion parameter for different feedstocks (cf. Fig. 10). In hindsight, one may calculate for Kuwait VGO ($P = 35\%$) a value of $Pe = 14$, which is the same as that obtained earlier from the fitting of actual experimental data.

It now remains to examine the decay of the mid-boiling temprerature T_{50} for different feedstocks. The detailed kinetic model simulations for varying feedstocks also yield information on T_{50} at any space time. In general one should except the rate of decay of T_{50} (or, equivalently, the mean molecular weight) to depend on the magnitude of T_{50} (i.e. on the size of the "average" molecule). Assume therefore the general nth-order dependence for the decay:

$$\frac{d\left(\frac{T_{50,\tau}}{T_{50,f}}\right)}{d\tau} = -k_{50}\left(\frac{T_{50,\tau}}{T_{50,f}}\right)^n. \quad (5)$$

For a wide range of feedstock composition and boiling point distribution the decay order, n, along with the corresponding decay rate constant k_{50}, have been plotted in Fig. 11 as a function of the feed paraffinicity. It is observed, as in the case of the dispersion parameter, that n and k_{50} are practically independent of the naphthene/aromatic ratio in the feed as well as the TBP of the feed. For the range of practical interest the following simple correlations for the decay order and decay constant are found:

$$n = 1.9 - 0.015(\text{wt \% paraffins in feed}) \quad (6)$$

and

$$k_{50} = 0.4 - 0.003(\text{wt \% paraffins in feed}). \quad (7)$$

The decay order, n, is seen to vary from nearly second-order for extremely low paraffinic feeds to approximately first-order for richly paraffinic feeds. This is quite an expected behaviour in view of the higher reduction in the crackability of aromatics and naphthenes with the reduction in their molecular weights compared to that of paraffins (Tom *et al.*, 1972). For Kuwait VGO ($P = 35\%$) it is found from eq. (6) that $n = 1.375$, only slightly higher than the earlier assumed decay order of unity (cf. Fig. 3). Interestingly, Strangeland (1974), using his model based on comminution, had also concluded that the model parameters for description of the TBP curves were dependent largely on the feedstock paraffinicity.

CONCLUSIONS

A new approach has been developed for the description of the kinetics of hydrocracking which draws an analogy between cracking (alteration of the molecular weight distribution) and physical dispersion. The developed model has three parameters: Pe, n and k_{50}; for a given catalyst and set of operating conditions these three parameters have been found to be largely dependent on the paraffin content of the feedstock. The Peclet number describes the boiling point distributions around T_{50} and may be considered to reflect the "selectivity" of the catalyst for a given freedstock and set of operating conditions. The decay order of T_{50}, n, along with the decay constant, k_{50}, reflects the

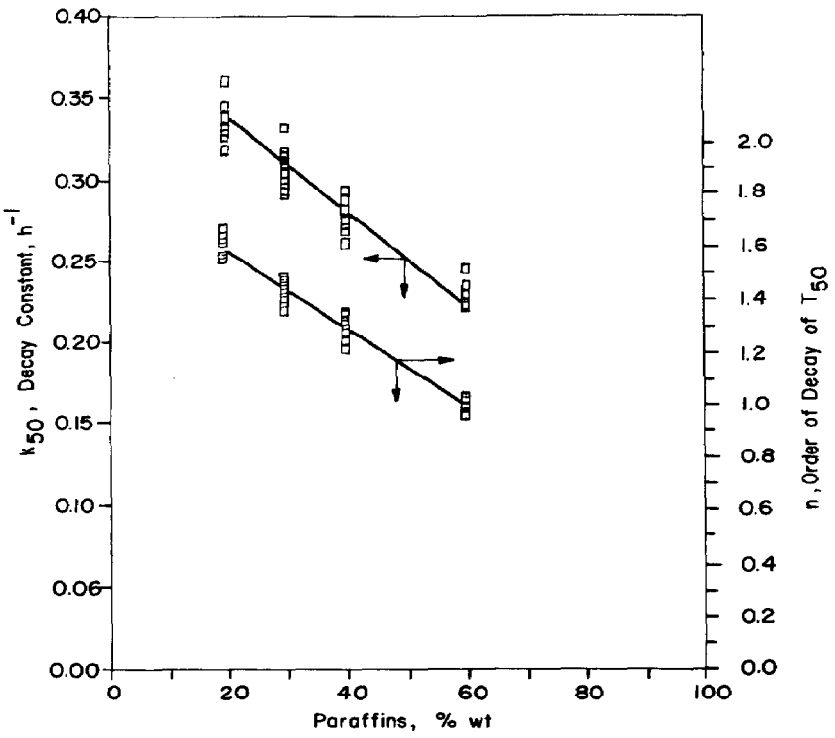

Fig. 11. Dependence of T_{50} decay order, n, and decay constant, k_{50}, on feedstock paraffinicity.

ease, or difficulty, with which the chosen catalyst will crack the particular feedstock, and these two parameters, together, portray the "'activity" of the catalyst.

Though the discussions have concentrated on hydrocracking, the procedure adopted here should apply equally well for catalytic cracking for which lumped kinetic models have been used [e.g. Nace *et al.* (1971)].

A further point to emphasize is that the model developed here does not consider thermal effects (such as temperature increases due to exothermic hydrocracking reactions) explicitly. Further study will be required in this regard before *a priori* predictions can be attempted. For the moment what has been achieved is a simple model, with a physical background, which could serve as a correlative tool for laboratory and pilot plant data, and in a limited sense for scale-up purposes.

NOTATION

A_H, A_L	wt % aromatics in T_{cut}^+ and T_{cut}^- fraction, respectively
f	fraction of material in product which boils below the specified temperature
FBP_f	feed final boiling point, °F or °C
$k_0 \ldots k_{10}$	lumped first-order constants for the kinetic scheme portrayed in Fig. 4
k_{50}	decay constant for reduction of T_{50}, h^{-1}
n	order of T_{50} decay
N_H, N_L	wt % naphthenes in T_{cut}^+ and T_{cut}^- fraction, respectively
Pe	Peclet number for axial-dispersion model [eq. (2)]
P_H, P_L	wt % paraffins in T_{cut}^+ and T_{cut}^- fraction, respectively
RMSD	root mean square deviation
S_C	wt % sulphur compounds
T^*	normalized dimensionless temperature according to eq. (1)
T_{50}	mid boiling temperature, °F
$T_{50,f}$	mid boiling temperature of feed, °F or °C
T_{cut}	cut temperature, °F or °C
TBP	true boiling point, °F or °C

Greek letter

τ	space time, h

Subscripts

0	at zero space time (i.e. feed)
f	pertaining to feed
τ	at space time τ

REFERENCES

Bennett, R. N. and Bourne, K. H., 1972, Hydrocracking for middle distillate—a study of process reactions and corresponding product yields and qualities, in *Symposium on Advances in Distillate and Residual Oil Technology*, presented at the Division of Petroleum Chemistry, American Chemical Society, New York, 27 August–1 September 1972, pp. G45–G62.

Langlois, G. E. and Sullivan, R. F., 1969, Chemistry of hydrocracking, in *Symposium on Refining Petroleum for Chemicals*, presented at the Division of Petroleum Chemistry and the Division of Industrial and Engineering Chemistry, American Chemical Society, New York, 7–12 September 1969, pp. D18–D39.

Maxwell, J. B., 1965, *Data Book on Hydrocarbons; Application to Process Engineering*, 8th Edition. D. Van Nostrand, New York.

Nace, D. M., Voltz, S. E. and Weekman, V. W., 1971, Application of a kinetic model for catalytic cracking. *Ind. Engng Chem. Process Des. Dev.* **10**, 530–541.

Smith, J. M., 1981, *Chemical Engineering Kinetics*, 3rd Edition. McGraw-Hill, New York.

Strangeland, B. E., 1974, A kinetic model for the prediction of hydrocracker yields. *Ind. Engng Chem. Process Des. Dev.* **13**, 71–76.

Tom, T. B., Mosby, J. F. and Gutberlet, L. C., 1972, Hydrocracking for distillates, in *Symposium on Advances in Distillate and Residual Oil Technology*, presented at the Division of Petroleum Chemistry, American Chemical Society, New York, 27 August–1 September 1972, pp. G4–G15.

APPENDIX A: SOLUTION OF RATE EQUATIONS

For the case of isothermal conditions, the rate equations for the kinetic model given in Fig. 4 were analytically solved to describe the weight percent of each lump as a function of space time (τ). The solution can be given as

$$S_C = S_{C0}\exp(-k_0\tau)$$

$$A_H = a_1\exp(-k_0\tau)+a_2\exp[-(k_1+k_2+k_3+k_4+k_5)\tau]$$

$$N_H = a_3\exp(-k_0\tau)+a_4\exp[-(k_1+k_2+k_3+k_4+k_5)\tau]+a_5\exp[-(k_6+k_7)\tau]$$

$$P_H = a_6\exp(-k_0\tau)+a_7\exp[-(k_1+k_2+k_3+k_4+k_5)\tau]+a_8\exp[-k_8\tau]$$

$$A_L = a_9\exp(-k_0\tau)+a_{10}\exp[-(k_1+k_2+k_3+k_4+k_5)\tau]+a_{11}\exp(-k_9\tau)$$

$$N_L = a_{12}\exp(-k_0\tau)+a_{13}\exp[-(k_1+k_2+k_3+k_4+k_5)\tau]+a_{14}\exp[-(k_6+k_7)\tau]+a_{15}\exp(-k_9\tau)+a_{16}\exp(-k_{10}\tau)$$

$$P_L = 100-S_C-A_H-N_H-P_H-A_L-N_L$$

where

$$a_1 = k_0 S_{C0}/(k_1+k_2+k_3+k_4+k_5-k_0)$$

$$a_2 = A_{H0}-a_1$$

$$a_3 = k_1 a_1/(k_6+k_7-k_0)$$

$$a_4 = k_1 a_2/(k_6+k_7-k_1-k_2-k_3-k_4-k_5)$$

$$a_5 = N_{H0}-a_3-a_4$$

$$a_6 = k_3 a_1/(k_8-k_0)$$

$$a_7 = k_3 a_2/(k_8-k_1-k_2-k_3-k_4-k_5)$$

$$a_8 = P_{H0}-a_6-a_7$$

$$a_9 = k_2 a_1/(k_9-k_0)$$

$$a_{10} = k_2 a_2/(k_9-k_1-k_3-k_4-k_5)$$

$$a_{11} = A_{L0}-a_9-a_{10}$$

$$a_{12} = (k_5 a_1+k_6 a_3+k_9 a_9)/(k_{10}-k_1-k_2-k_3-k_4-k_5)$$

$$a_{13} = (k_5 a_2+k_6 a_4+k_9 a_{10})/(k_{10}-k_1-k_2-k_3-k_4-k_5)$$

$$a_{14} = k_6 a_5/(k_{10}-k_6-k_7)$$

$$a_{15} = k_9 a_{11}/(k_{10}-k_9)$$

$$a_{16} = N_{L0}-a_{12}-a_{13}-a_{14}-a_{15}.$$